The Journal of Neuroscience, April 1988, 8(4): 1400–1410

Stratum Lacunosum-Moleculare Interneurons of Hippocampal CA1 Region. I. Intracellular Response Characteristics, Synaptic Responses, and Morphology

Jean-Claude Lacaille[1,a] and Philip A. Schwartzkroin[1,2]

Departments of [1]Neurological Surgery and [2]Physiology and Biophysics, University of Washington, Seattle, Washington 98195

Stable intracellular recordings were obtained from nonpyramidal cells (interneurons) in stratum lacunosum-moleculare (L-M) of the CA1 region of guinea pig hippocampal slices. The intracellular response characteristics of these interneurons were distinctly different from responses of pyramidal cells and of other interneurons (basket cells and oriens-alveus interneurons). L-M interneurons had a high resting membrane potential (−58 mV), a high input resistance (64 MΩ), and a large amplitude (60 mV), relatively long duration (2 msec) action potential. A large afterhyperpolarization (11 mV, 34 msec) followed a single action potential. Most L-M interneurons did not display any spontaneous firing.

Lucifer yellow (LY)-filled L-M interneurons showed nonpyramidal morphology. Cells were generally fusiform or multipolar, with aspinous, beaded dendritic processes ramifying in stratum lacunosum-moleculare, radiatum, and (sometimes) oriens. The varicose axon originated from a primary dendrite, projected along stratum lacunosum-moleculare, branched profusely in stratum radiatum, and coursed toward and into stratum pyramidale and occasionally into oriens. Processes of cells with somata in the L-M region of CA1 were not restricted to the CA1 region. The dendritic and axonal processes of some L-M interneurons were seen ascending in stratum lacunosum-moleculare, crossing the hippocampal fissure, and coursing in stratum moleculare of the dentate gyrus.

Excitatory and inhibitory postsynaptic potentials (EPSPs and IPSPs) were evoked in L-M interneurons from stimulation of major hippocampal afferents. EPSPs were most effectively elicited by stimulation of fiber pathways in transverse slices, whereas IPSPs were predominantly evoked when major pathways were stimulated in longitudinal slices.

We have identified a population of interneurons with intracellular response characteristics and morphology distinctly different from previously described pyramidal and nonpyramidal neurons of CA1 region. The possible role of these interneurons in hippocampal circuitry is discussed.

The anatomy of local circuit neurons (interneurons) was first described in the Golgi studies of Ramon y Cajal (1911) and Lorente de No (1934). More recent studies also suggest a great diversity of hippocampal interneuron types (Amaral, 1978; Somogyi et al., 1983). Some information about the physiology of the various interneuron cell types, and about the way in which they influence neurotransmission through the principal trisynaptic circuit of the hippocampal formation, has also been forthcoming (Andersen et al., 1969; Knowles and Schwartzkroin, 1981; Buzsaki and Eidelberg, 1982; Ashwood et al., 1984; Lacaille et al., 1987).

Using the hippocampal slice preparation, intracellular recordings have been obtained from 2 types of interneurons of the CA1 region. These are the so-called basket cells located at the border of strata pyramidale and oriens (Schwartzkroin and Mathers, 1978; Knowles and Schwartzkroin, 1981; Ashwood et al., 1984), and the oriens/alveus (O/A) interneurons situated at the junction of stratum oriens and the alveus (Lacaille et al., 1987). Both types of interneurons have intracellular response characteristics that are very different from pyramidal cell responses but that are similar to each other. In contrast to pyramidal cells, they display a high spontaneous discharge rate, a short duration action potential, and a pronounced action potential afterhyperpolarization; they respond with a nonaccommodating burst of action potentials to a depolarizing current pulse. Morphologically, these cells are distinctly nonpyramidal (Schwartzkroin and Mathers, 1978; Schwartzkroin and Kunkel, 1985; Lacaille et al., 1987) and appear similar to interneurons that are immunoreactive for GABA (Gamrani et al., 1986) and glutamic acid decarboxylase (GAD) (Ribak et al., 1978; Kunkel et al., 1986). Simultaneous intracellular recordings from pairs of interneurons and pyramidal cells showed that pyramidal cells could directly excite both types of interneurons and, in turn, these interneurons could directly inhibit pyramidal cells (Knowles and Schwartzkroin, 1981; Lacaille et al., 1987). In addition, these interneurons were directly excited by major hippocampal afferents so that their inhibitory action on pyramidal cells could occur in a feedforward manner (Knowles and Schwartzkroin, 1981; Lacaille et al., 1987). Following intracellular HRP injections and processing for electron microscopy, basket cell and O/A interneuron axons were found to make Type II symmetric

Received Apr. 7, 1987; revised Sept. 18, 1987; accepted Sept. 28, 1987.

This work was supported by National Institutes of Health, National Institute of Neurological and Communicative Disorders and Stroke Grants NS 15317 and NS 18897. J.-C.L. was partially supported by a NATO Science Fellowship from the Natural Sciences and Engineering Research Council of Canada and by a Postdoctoral Fellowship from Fonds de la Recherche en Santé du Québec. P.A.S. is an affiliate of the Child Development and Mental Retardation Center, University of Washington.

Correspondence should be addressed to Professor Philip A. Schwartzkroin, Department of Neurological Surgery, RI-20, University of Washington, School of Medicine, Seattle, WA 98195.

[a] Present address: Département de physiologie, Centre de recherche en sciences neurologiques, Faculté de Médecine, Université de Montréal, Montréal, Québec, Canada H3C 3J7.

synaptic contacts, characteristic of inhibitory synapses, onto CA1 pyramidal cells (Schwartzkroin and Kunkel, 1985; Lacaille et al., 1987). Thus, based on anatomical and physiological evidence, both basket and O/A interneurons appear to mediate feedforward and feedback inhibition of CA1 pyramidal cells.

To further elucidate the role of interneurons in hippocampal function we have applied similar intracellular recording and anatomical methods to interneurons located in stratum lacunosum-moleculare (L-M interneurons), near the stratum radiatum border of CA1 region in guinea pig hippocampal slices. This paper reports their intracellular response characteristics, their intracellular responses to electrical stimulation of major hippocampal afferents, and their morphology following intracellular injection of Lucifer yellow (LY).

Materials and Methods

Slices. Hippocampal slices were obtained from Hartley guinea pigs (200–300 gm) as described previously (Schwartzkroin, 1975, 1981; Lacaille et al., 1987). Briefly, the animal was decapitated and the hippocampus rapidly dissected out. Five hundred micron thick slices were cut on a McIlwain tissue chopper. For transverse slices, the hippocampus was cut perpendicularly to its septotemporal axis. For longitudinal slices, septal and temporal thirds were cut out transversely, and the remaining middle third was sliced parallel to its longitudinal axis. Slices were transferred to a nylon net of a gas–fluid interface chamber, where their undersurfaces were bathed in artificial cerebrospinal fluid (ACSF) and their upper surfaces were exposed to a warmed, humidified atmosphere (95% O_2–5% CO_2). The ACSF consisted of (in mM): NaCl, 124; KCl, 5; NaH_2PO_4, 1.25; $MgSO_4$, 2; $CaCl_2$, 2; $NaHCO_3$, 26; and dextrose, 10. The ACSF was continuously oxygenated (95% O_2–5% CO_2), heated to 35.5 ± 0.5°C, and perfused at a rate of 1 ml/min.

Intracellular recordings. Micropipettes (50–100 MΩ) were pulled from capillary-filled borosilicate glass tubing on a Brown-Flaming puller and filled with 4 M potassium acetate and 0.01 M KCl. To obtain interneuron intracellular recordings, the micropipette was placed under visual guidance in stratum lacunosum-moleculare near the border of stratum radiatum. Stratum lacunosum-moleculare could be easily distinguished from stratum radiatum by its greater opaqueness, which is due to the higher density of myelinated fibers. The microelectrode was lowered through the slice with a hydraulic stepping microdrive (Kopf). Stable intracellular recordings (15 min–3 hr) were obtained from neurons in stratum L-M. Only very rarely could stable recordings be obtained from pyramidal cell dendrites in L-M, and such recordings could be easily distinguished from interneuron recordings. In intradendritic recordings, the electrode resistance increased substantially upon penetration, and relatively small-amplitude, long-duration spike-like events were evoked by depolarizing current injection. Following stabilization of the penetration, large-amplitude, short-duration action potentials were evoked during depolarizing current pulses. Fractionated spikes and large bursts were produced with higher current intensities, as previously reported by others (Wong et al., 1979). Intracellular staining (with LY) of presumed pyramidal cell dendrites confirmed these characteristics of intradendritic recordings.

Intracellular signals were amplified with a NeuroData dual-channel intracellular amplifier (IR-283), displayed on a cathode ray oscilloscope, digitized with a NeuroCorder (DR-484), and stored on digital tape for later retrieval and analysis with a microcomputer (Norland 3001/DMX). Intracellular stimulation (0.1–1.0 nA, 50 or 100 msec pulses) was carried out with a bridge circuit. Bipolar electrical stimulation of afferent fibers was done with resin-coated electrolytically etched tungsten microelectrodes, placed under visual guidance, using constant-current pulses (50 μsec duration, 0.05–0.5 nA).

Measurement of membrane characteristics. When a stable intracellular recording was obtained, the neuron was characterized electrophysiologically (for example, see Fig. 1). Action potential amplitude was measured as the difference between resting membrane potential and the peak of the action potential. Duration of the action potential was measured at its base. Resting membrane potential was determined as the potential change upon withdrawal of the electrode from the cell. Amplitude of the spike afterhyperpolarization was taken as the amplitude difference between the base of the action potential and the peak of the hyperpolarization following the spike; duration of the spike afterhyperpolarization was measured as the time between the point at which the repolarizing action potential crossed resting membrane potential and the point at which the post-spike membrane potential recovered to resting potential. Amplitude of the burst afterhyperpolarization was taken as the amplitude difference between resting potential and the peak of the hyperpolarization that followed a 100 msec, 0.5 nA intrasomatic depolarizing current pulse; duration of the burst afterhyperpolarization was measured as the time difference between the offset of the depolarizing current pulse and the recovery to baseline of the hyperpolarizing membrane potential. Spontaneous firing rate was measured at resting membrane potential. Time constant of the cell was calculated with a 50 msec, 0.5 nA hyperpolarizing current pulse as the time necessary to reach $1\text{-}e^{-1}$ (63%) of the maximum voltage deflection. Input resistance of the cell was measured from the current–voltage plot constructed from a series of current pulses of varying intensity (0 to −1 nA in 0.1 nA steps); the maximum voltage deflection was measured at each current intensity (2 trials) and plotted as a function of injected current. For each cell, the input resistance was taken as the slope of the linear regression line passing through the origin.

Intracellular LY injection. The morphology of some cells was examined with intracellular LY injections following their electrophysiological characterization. In these cases, the recording electrode was filled with 4% LY (Lucifer yellow CH, Aldrich) in 1 M LiCl (Stewart, 1978, 1981; Lacaille et al., 1987). The dye was injected intracellularly by passing steady hyperpolarizing current through the recording electrode (−0.5 to −1.0 nA for 5–10 min). Only one cell was injected per slice. After injection of LY, the electrode was withdrawn from the cell, and the slide remained undisturbed in the chamber for 10 min. Then it was removed and placed between 2 filter papers in a petri dish containing the fixative 3% paraformaldehyde lysine periodate (PLP; Kunkel et al., 1986). Following 2–4 hr of fixation, slices were transferred to phosphate buffer (PB; 0.1 M, pH 7.4). Prior to sectioning, they were sunk in 30% sucrose PB. Slices were then frozen and cut on a freezing microtome. Sections (30–70 μm thick) were cleared in a series of alcohols, air-dried, and coverslipped in glycerol in propyl gallate (5%). The sections were then examined and photographed on a Leitz Dialux 20 epifluorescence microscope equipped with the appropriate filters. Major hippocampal subdivisions (strata oriens, pyramidale, radiatum, lacunosum-moleculare, hippocampal fissure, and stratum moleculare of dentate gyrus) were easily seen under the fluorescence microscope. To assist with localization of the stained neuron within CA1 region, drawings were made of the interneurons and their processes, identifying their position within the hippocampus. Interneurons with cellular processes in adjacent sections were occasionally reconstructed from photographs of serial sections by tracing the outline of the neuronal processes from the projected negatives.

Results

Intracellular membrane characteristics

Because of the small number of neurons in stratum lacunosum-moleculare, stable impalements from interneurons in this layer were much less frequent than from pyramidal cells and other interneurons at the pyramidale/oriens border or at the O/A border. Stable impalements were obtained from 43 interneurons in stratum lacunosum-moleculare, and their intracellular responses were characterized electrophysiologically. The mean and range of these membrane characteristics for all recorded cells are listed in Table 1. These cells had a mean resting membrane potential of −58.3 mV. The majority of cells did not fire action potentials spontaneously; spontaneously active interneurons (16 of 42) had a mean firing rate of 10.2 Hz. The mean action potential amplitude of lacunosum-moleculare interneurons was 60.1 mV, and the mean action potential duration was 2.0 msec. These interneurons had a high input resistance (mean, 63.7 MΩ) and a mean time constant of 8.6 msec. A conspicuous feature was their large spike afterhyperpolarization (mean amplitude, 10.8 mV; mean duration, 34.4 msec). In response to a depolarizing current pulse (0.5 nA, 100 msec), the cells fired an average 7.2 action potentials. In 31 of 42 interneurons, a late

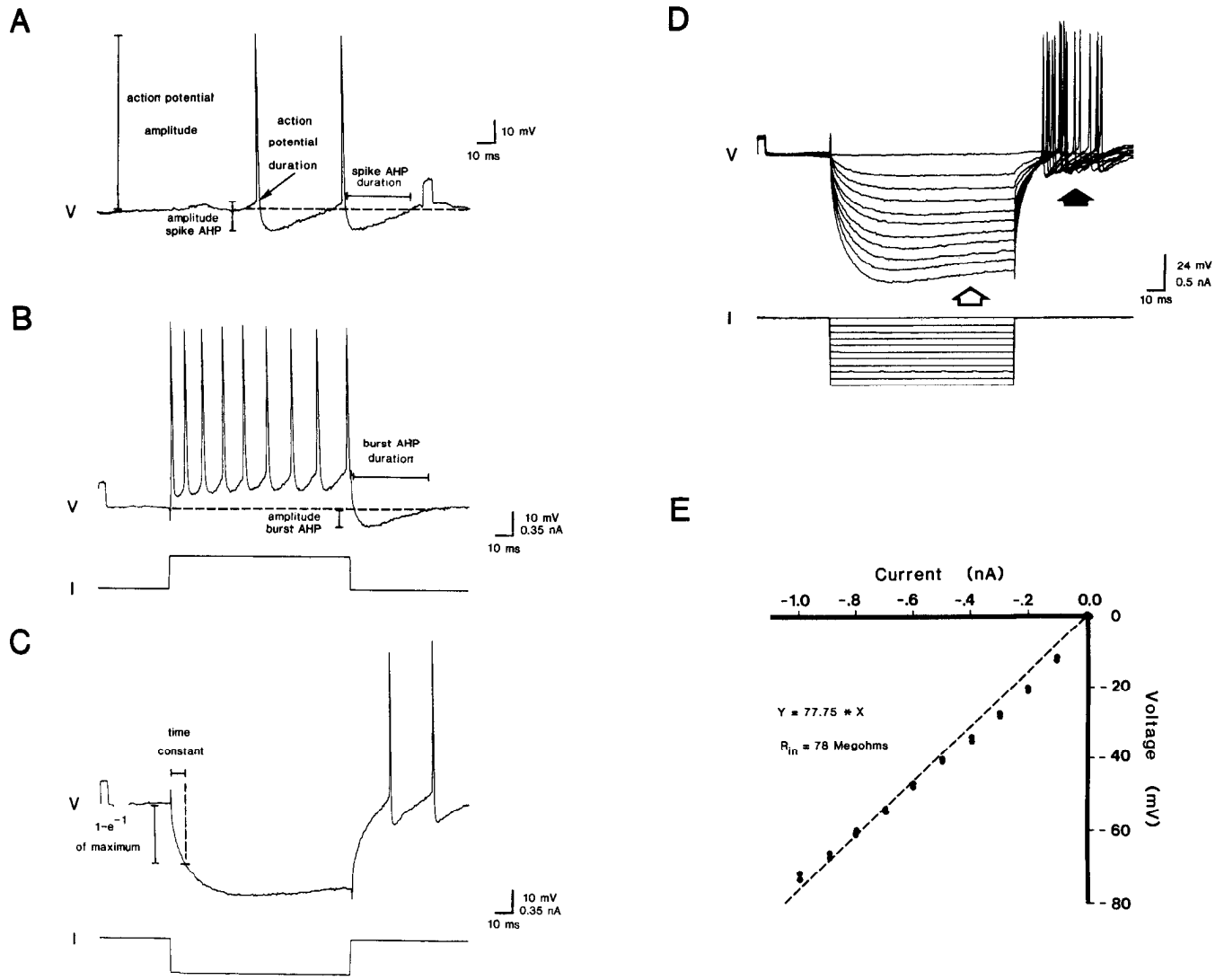

Figure 1. Membrane characteristics of a typical lacunosum-moleculare interneuron (resting potential, −59 mV). *A*, Spontaneous action potentials. Note the pronounced spike afterhyperpolarization. See Materials and Methods for explanation of measured characteristics. *B*, Burst of action potentials evoked by an intracellular 0.5 nA depolarizing current pulse. Note that there is little frequency adaptation during the current-evoked burst. In contrast to most cells, there is only a small burst afterhyperpolarization in this cell (which is probably a spike AHP). *C*, Intracellular response to a 0.5 nA hyperpolarizing current pulse used to measure the time constant. Note the rebound excitation at pulse offset. *D*, Eleven superimposed traces showing the intracellular responses to hyperpolarizing current pulses (0–1 nA in steps of 0.1 nA). Note the sag in the response to higher current intensities (*open thick arrow*) and the anode break excitation (*filled thick arrow*). *E*, *I–V* curve constructed from maximum voltage deflections evoked by the series of hyperpolarizing pulses in *C*. *Broken line* is a linear regression passing through the origin; input resistance is taken from the slope of the line. Note that the data points deviate somewhat from a straight line, indicating that some membrane rectification occurs within this voltage range.

afterhyperpolarization (mean amplitude, 5.4 mV; mean duration 241.8 msec) followed this burst of action potentials. Lacunosum-moleculare interneurons lacked the high-frequency spontaneous synaptic potentials characteristic of basket cells and O/A interneurons (Schwartzkroin and Mathers, 1978; Knowles and Schwartzkroin, 1981; Lacaille et al., 1987).

The intracellular electrophysiological responses of an L-M interneuron, representative of the mean responses, are shown in Figure 1. This cell had a resting membrane potential of −59 mV and fired spontaneously at 8.5 Hz (Fig. 1*A*). The action potential amplitude was 71 mV, and spike duration was 1.8 msec. The spike afterhyperpolarization amplitude measured 12 mV and the duration 35 msec (Fig. 1*A*). This cell fired 9 action potentials in response to the depolarizing current pulse (0.5 nA, 100 msec; Fig. 1*B*). Although not a prominent feature, it can be seen that some frequency accommodation is present in the repetitive discharge of this cell; Figure 1*B* shows that the interval between successive action potentials widens during the burst. Contrary to most cells, this interneuron does not display a burst afterhyperpolarization following this burst (the afterhyperpolarization seen is a *spike* afterpotential). The response of this cell to a −0.5 nA hyperpolarizing current pulse is shown in Figure 1*C*. From this voltage response a time constant of 6.7 msec was obtained. As in the majority of cells, a small "sag" is seen in the voltage response during the hyperpolarization, and an above threshold depolarizing response follows the offset of the current pulse (anodal break excitation; Fig. 1*C*). This membrane rectification is also evident in Figure 1*D* in the responses

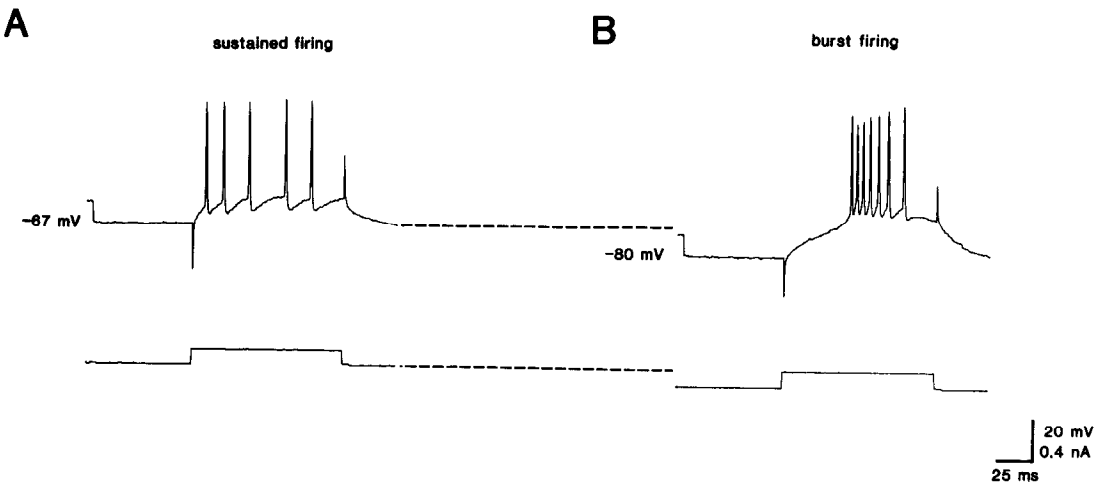

Figure 2. Voltage-dependent mode of firing. *A*, Depolarizing current pulse (0.1 nA, 100 msec) evoked a sustained train of 5 action potentials when delivered at normal resting membrane potential. *B*, Similar depolarizing current pulse (0.1 nA, 100 msec) evoked a rapidly accommodating burst of 7 action potentials when the membrane was hyperpolarized with steady DC current (−0.1 nA). For this cell, RMP = −67 mV, R_{in} = 88 MΩ.

to the higher intensity current pulses (−0.4 to −1 nA). A current–voltage graph constructed from 2 series of hyperpolarizing current pulses is shown in Figure 1*E*. The broken line represents the linear regression equation passing through the origin; the slope of the line yields an input resistance of 78 MΩ for this cell. It is also evident from this graph that the cell membrane does not behave in a strictly ohmic fashion within this voltage range and that some rectification takes place. Such rectification was seen in the majority of L-M cells.

A characteristic often observed in L-M interneurons was a differential mode of action potential discharge, determined by resting membrane potential. As illustrated in Figure 2*A*, a depolarizing current pulse given at normal resting membrane potential evoked a sustained train of action potentials. However, application of the same depolarizing current pulse when the membrane was hyperpolarized (−13 mV from rest) now evoked a rapidly adapting burst of action potentials (Fig. 2*B*).

Morphology following intracellular LY injection

Sixteen electrophysiologically identified lacunosum-moleculare interneurons were recovered following intracellular injection of LY. Morphologically, these neurons were clearly nonpyramidal (Fig. 3*A–C*, 3 different interneurons) and formed a relatively homogenous group of neurons. The somata were situated in stratum lacunosum-moleculare, near the stratum radiatum border. In general, the cells were fusiform and multipolar, approximately 20 μm in diameter (Fig. 3). Four of 16 neurons appeared fusiform and bipolar. In 11 neurons, the dendrites could be followed for relatively long distances, with the total dendritic tree sometimes spanning two-thirds of the CA1 region. The dendrites were mostly smooth and beaded (Fig. 3*C*). These dendrites radiated out from the soma along stratum lacunosum-moleculare; after a short distance, some turned into stratum radiatum, where they branched (Fig. 3). In 4 cells, some dendrites crossed the pyramidal cell layer and entered stratum oriens (e.g., Fig. 3, *A, C*). In some interneurons the dendritic processes ran for great distances and expanded outside the CA1 region. For 3 such cells some dendritic branches could be followed ascending in stratum lacunosum-moleculare, crossing the hippocampal fissure and projecting into the dentate gyrus molecular layer (e.g., Fig. 3, *A, C*).

In 5 L-M interneurons, the LY-filled axon was visualized. The axon usually started out from a primary dendrite in stratum lacunosum-moleculare (arrow, Fig. 3*C*). It had a varicosed, or

Table 1. Membrane characteristics of lacunosum-moleculare interneurons

Characteristic	Mean	SD	Range	*n*
Resting membrane potential (mV)	−58.3	11.3	−31, −86	43
Action potential amplitude (mV)	60.1	12.2	30, 78	43
Action potential duration (mV)	2.0	0.7	0.9, 4.0	43
Input resistance (MΩ)	63.7	27.9	21, 144	43
Time constant (msec)	8.6	5.3	2.8, 28.4	42
Spontaneous firing rate (Hz, positive cells only)	10.2	10.9	0.5, 48.4	16
Number of action potentials per 0.5 nA current pulse	7.2	2.8	1, 15	43
Afterhyperpolarization amplitude, single spike (mV)	10.8	4.0	3.8, 21.7	43
Afterhyperpolarization duration, single spike (msec)	34.4	20.2	8, 80	37[a]
Afterhyperpolarization amplitude, burst (mV, positive cells only)	5.4	2.1	1.9, 10.0	31
Afterhyperpolarization duration, burst (msec, positive cells only)	241.8	223	54, 1088	31

[a] In 6 cells the duration of single spike AHP could not be accurately measured.

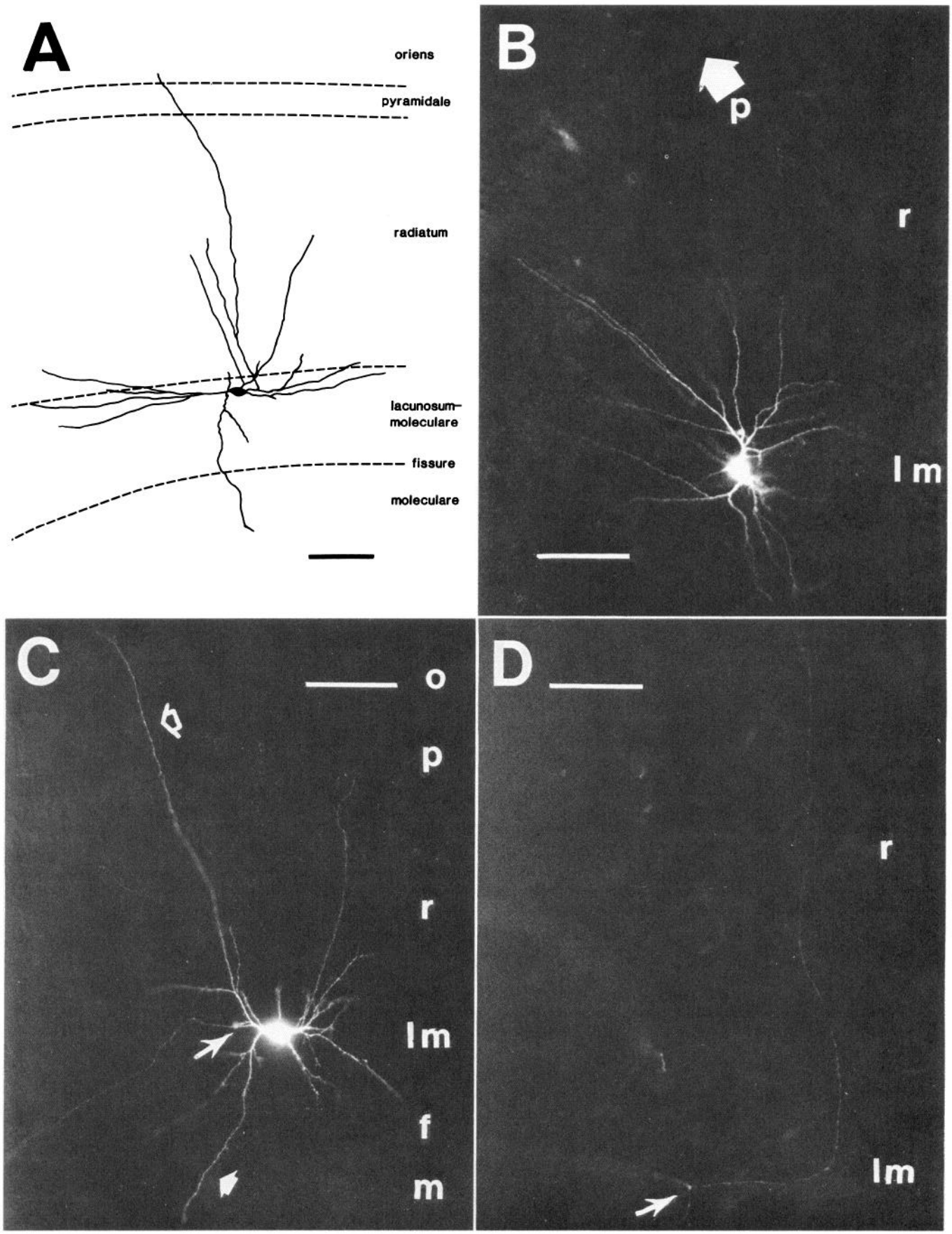

Figure 3. Morphology of 3 electrophysiologically identified L-M interneurons. *A,* Reconstruction from fluorescence micrographs of a LY-filled interneuron. All cells recorded from were similarly located at the radiatum border of stratum lacunosum-moleculare. Note multipolar soma, and

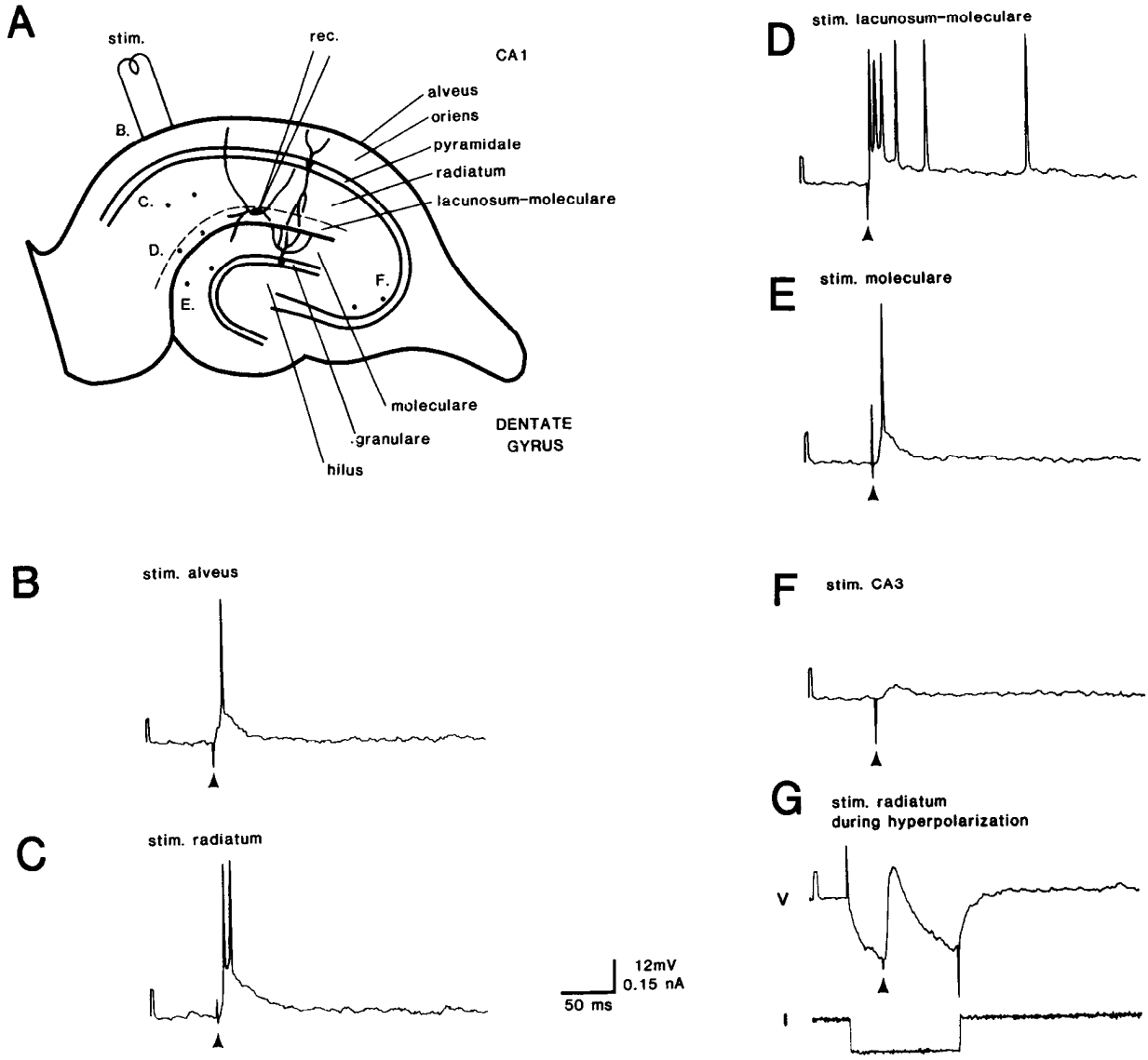

Figure 4. Synaptic responses of a lacunosum-moleculare interneuron to stimulation of major hippocampal afferents in a transverse slice. *A*, Diagram of transverse slice with electrode placements. *B*, Electrical stimulation of alveus (*arrowhead*, 0.5 mA, 0.05 msec) evokes an EPSP that triggers an action potential. *C*, Stimulation of stratum radiatum (*arrowhead*, 0.1 mA, 0.05 msec) produces a greater EPSP that evokes 2 action potentials. *D*, Stimulation of stratum lacunosum-moleculare (*arrowhead*, 0.3 mA, 0.05 msec) evokes a longer-lasting EPSP that produces 6 action potentials. *E*, Stimulation of molecular layer of the dentate gyrus (*arrowhead*, 0.4 mA, 0.05 msec) also produces an EPSP that triggers an action potential. *F*, Stimulation of stratum radiatum of the CA3 region (*arrowhead*, 0.5 mA, 0.05 msec) evokes a small EPSP that fails to reach threshold. *G*, Stimulation of stratum radiatum as in *C* (*arrowhead*) but applied during hyperpolarization (100 msec, −0.15 nA) of the membrane evokes an EPSP of increased amplitude (indicating a "convential" EPSP with reversal potential positive to the resting membrane potential). Resting membrane potential for this cell was −52 mV; input resistance, 56 MΩ; action potential amplitude, 50 mV.

beaded, appearance (Fig. 3*D*) and often projected for long distances along the L-M layer; in transverse slices, the axon could be seen running to the subicular or the CA3 border. In all instances, the axon branched shortly after emerging from the dendrite and projected into stratum radiatum (in plane of focus of Fig. 3*C*, axonal processes appear faintly in the background). The axon was also seen projecting into and along stratum pyramidale and occasionally entering into stratum oriens. Axonal processes

←

dendritic processes radiating into strata lacunosum-moleculare, radiatum and oriens. Also note a dendritic process ascending in stratum lacunosum-moleculare, crossing hippocampal fissure, and entering stratum moleculare of dentate gyrus. *B* and *C*, Fluorescence micrographs of different LY-filled L-M interneurons with similar morphologies. In *C* a dendrite (*open thick arrow*) descends through stratum oriens (*o*) to the alveus, and another dendrite (*filled thick arrow*) ascends in stratum lacunosum-moleculare (*lm*), crosses the hippocampal fissure (*f*), and enters stratum moleculare (*m*) of dentate gyrus. Also in *C*, the axon takes off from a primary dendrite (*arrow*); it branches in strata radiatum (*r*), pyramidale (*p*), and oriens. In this plane of focus, axon collaterals appear faintly in the background. *D*, Higher-power micrograph of varicose axon of interneuron in *C*, approximately 500 μm away from the soma (to the right of soma in *C*, towards the CA3 region). The axon branches (*arrow*), with one collateral ascending toward the fissure and remaining axonal process abruptly turning and descending toward stratum pyramidale. Calibration bars: 100 μm in *A–C*, 40 μm in *D*.

projecting along stratum lacunosum-moleculare gave some collateral branches descending in stratum radiatum and others ascending toward the hippocampal fissure (Fig. 3*D*). Axonal projections of L-M interneurons were not restricted to the CA1 region. In 2 interneurons, axon collaterals crossed the hippocampal fissure and could be followed in the molecular layer of the dentate gyrus.

Synaptic responses in transverse slices

Synaptic potentials evoked by electrical stimulation of major hippocampal afferents were examined in 13 lacunosum-moleculare interneurons in transverse slices. In all cells, stimulation in the alveus, stratum oriens, pyramidale, radiatum, or lacunosum-moleculare evoked EPSPs (Fig. 4). Hyperpolarization of the membrane resulted in an increase in the amplitude of the EPSPs (Fig. 4, *G* vs. *C*). In most cases, EPSPs were of sufficient amplitude to produce one or more action potentials. In transverse slices, IPSPs were usually not observed.

The EPSPs evoked from different hippocampal layers varied in amplitude and duration. Although not quantitatively assessed, qualitative differences in synaptic efficacy were seen in most cells. In these experiments, bipolar stimulating electrodes were placed successively in major CA1 afferent pathways, and the maximal synaptic response evoked by stimulation of each pathway (0.05 msec, 0.1–0.3 mA) was recorded. As shown for a representative cell in Figure 4, the most effective site of stimulation was within stratum lacunosum-moleculare itself, where stimuli evoked an EPSP lasting more than 100 msec and producing 6 action potentials (Fig. 4*D*). Stimulation of stratum radiatum was the second most effective site, with the evoked EPSP lasting more than 50 msec and triggering 2 action potentials. Stimulation of the alveus was least effective, producing an EPSP lasting less than 50 msec and a single action potential.

In these experiments, distances between stimulation and recording sites were kept as constant as possible to avoid variations in distance that may contribute to differences in efficacy.

As shown in Figure 4*E*, stimulation of stratum moleculare of the dentate gyrus also evoked an EPSP of sufficient amplitude to produce an action potential in the L-M interneuron. In the cell illustrated here, dentate moleculare stimulation was as effective as stimulation of the alveus; however, in the majority of cells tested, dentate molecular stimulation was less effective. The synaptic response to dentate stimulation probably did not arise from activation of the granule cell–CA3 pyramidal cell–Schaffer collateral pathway, since (in the same cell) stimulation of stratum lucidum of the CA3 region was much less effective, producing a subthreshold EPSP one-third the amplitude of the dentate-evoked response. Thus, the synaptic responses evoked by dentate molecular stimulation probably were mediated by fibers in this layer, making excitatory synapses onto L-M interneuron dendrites that crossed the hippocampal fissure and arborized in the molecular layer.

Synaptic responses in longitudinal slices

Synaptic responses were examined in 5 L-M interneurons in longitudinal slices. In these experiments, following stable impalement and electrophysiological characterization, bipolar stimulating electrodes were placed successively in the alveus, strata oriens, radiatum, and lacunosum-moleculare. Synaptic responses evoked in longitudinal slices were very different from those elicited in transverse slices. At resting membrane potential, synaptic responses evoked from each hippocampal layer were usually multiphasic, with an initial IPSP followed by one or more depolarization–hyperpolarization sequences (Fig. 5*B2, C1, D1, E1*). These mainly inhibitory synaptic responses are in contrast to the mostly excitatory responses obtained in transverse slices (Fig. 4). We will refer to the late response component seen in the longitudinal slices as a depolarization–hyperpolarization sequence.

Occasionally, in longitudinal slices, the synaptic responses were even more complex than IPSP–depolarization–hyperpolarization sequence. First, with low-intensity stimulation, an early EPSP was sometimes intermixed with the early IPSP; often, it was of sufficient amplitude to evoke an action potential (Fig. 5*B1* alveus stimulation, and 5*D2* stratum radiatum). Second, in almost all cases, with sufficiently intense stimulation (within our "physiological" range), the depolarization following the IPSP was large enough to evoke an action potential (Fig. 5*B3, C2, E2*). Third, with high-intensity stimulation of stratum lacunosum-moleculare, an antidromic action potential could be evoked (Fig. 5*E3*); this antidromic action potential was evoked at a much shorter latency than the synaptically evoked action potential (in Fig. 5, *E3* antidromic spike latency 2.8 msec vs. *B1, D2* orthodromic spike latency 4.6–5.4 msec). Hyperpolarization of the membrane during stimulation of stratum lacunosum-moleculare at sufficient intensity to evoke an antidromic action potential did not uncover an underlying short-latency EPSP. Since stimulation of stratum lacunosum-moleculare more than 1000 μm away from the recorded cell sometimes evoked such a short-latency action potential, it seems likely the elicited spike was indeed antidromic and not directly activated in the soma by current spread.

To determine if the depolarization that followed the initial IPSP arose from a late synaptic EPSP or was due to intrinsic membrane properties, we stimulated the afferent fibers during hyperpolarization of the cell membrane. As shown in Figure 4*G*, hyperpolarization of the interneuron membrane during stimulation of transverse slices resulted in an EPSP of greater amplitude than the EPSP seen at resting potential. In longitudinal slices, stimulation of stratum oriens evoked an IPSP followed by a depolarization–hyperpolarization sequence sufficient to evoke an action potential at resting membrane potential (Fig. 6*A*). However, the same stimulation given during hyperpolarization of the membrane (with an intrasomatic current pulse of −0.4 nA, 200 msec) produced no observable synaptic potential (Fig. 6, *B, D*). The membrane here was hyperpolarized to the reversal potential of the IPSP. The depolarization that followed the IPSP in Figure 6*A* is absent (not increased in amplitude, as would a true EPSP). These results suggest that the late component of the synaptic response, the depolarization–hyperpolarization sequence, arises from intrinsic membrane properties activated by the IPSP. These intrinsic conductances could be similar to those resulting in the anode break excitation consistently seen in these same interneurons.

Discussion

We have obtained stable intracellular recordings from interneurons situated in stratum lacunosum-moleculare. Although there was some physiological and morphological variability from cell to cell, these interneurons appear to constitute a single cell population, different from other CA1 interneurons ("basket" cells and O/A interneurons) and different also from CA1 pyramidal cells. The distinctive membrane characteristics of the L-M interneurons make it possible, with intracellular record-

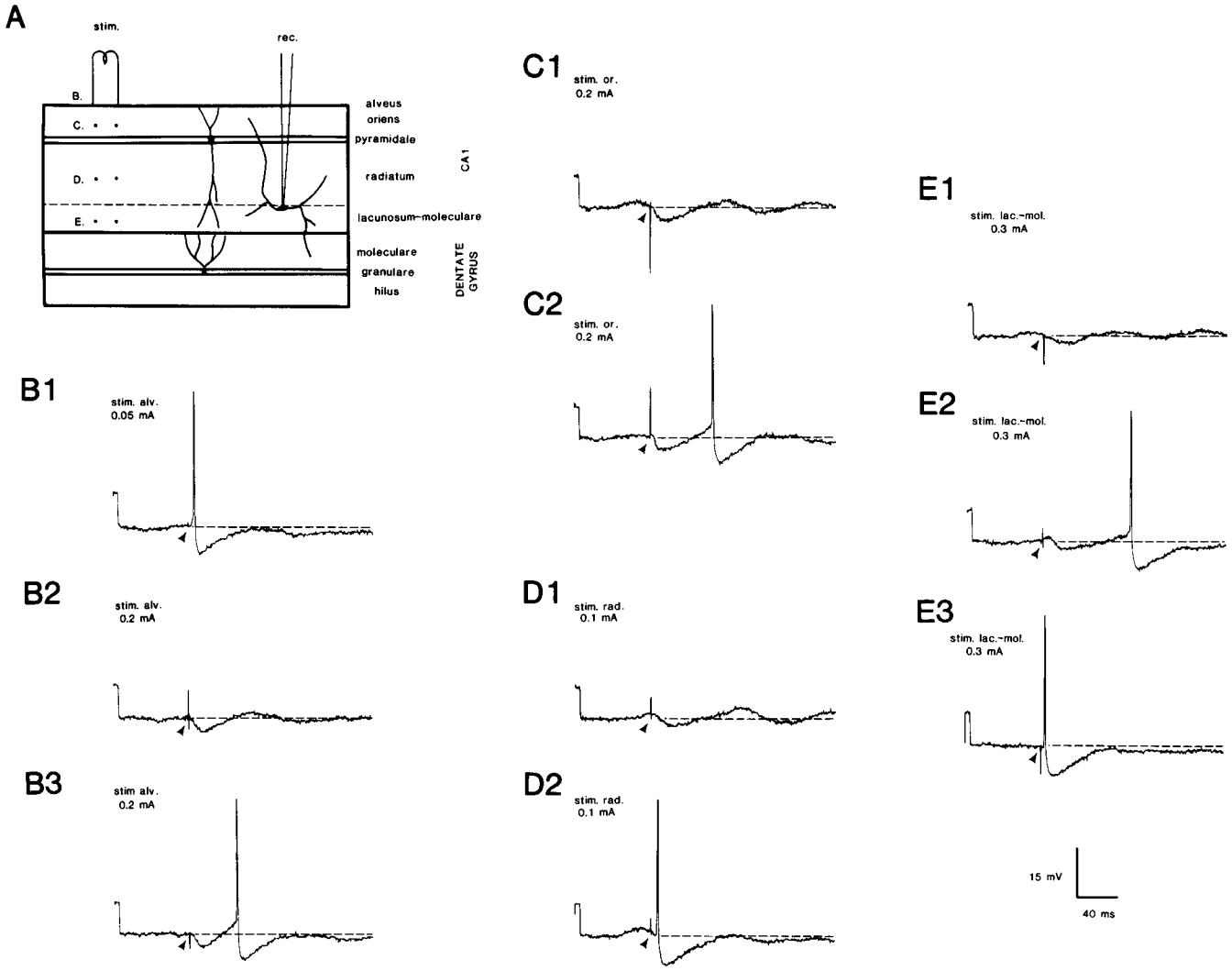

Figure 5. Synaptic responses of a lacunosum-moleculare interneuron to electrical stimulation of major hippocampal afferents in a longitudinal slice. *A,* Diagram of a longitudinal slice with electrode placements. *B,* Synaptic responses evoked by stimulation of the alveus (*arrowhead,* 0.5 msec). *B1,* Low-intensity stimulation (0.05 mA) evoked an EPSP that triggered a short latency action potential. *B2,* Higher-intensity stimulation evoked an IPSP followed by a depolarization–hyperpolarization sequence. *B3,* The depolarization that followed the IPSP was sufficient to trigger an action potential. *C,* Synaptic responses to stimulation of stratum oriens (*arrowhead,* 0.2 mA, 0.05 msec). *C1,* In this cell, a short latency action potential was not evoked at low-intensity stimulation; stimulation produced only an IPSP followed by a depolarization–hyperpolarization sequence. *C2,* The late depolarization was sometimes of sufficient amplitude to evoke an action potential. *D,* Synaptic responses to stimulation of stratum radiatum (*arrowhead,* 0.1 mA, 0.05 msec). *D1,* Stimulation usually produced an IPSP followed by sequences of depolarization–hyperpolarization. *D2,* Often an action potential was evoked from a short-latency EPSP. *E,* Responses to stimulation of stratum lacunosum-moleculare (*arrowhead,* 0.3 mA, 0.05 msec). *E1,* Synaptic responses usually consisted of an IPSP followed by depolarization–hyperpolarization sequences. *E2,* As with other stimulation sites, the late depolarization was often of sufficient amplitude to trigger an action potential. *E3,* Sometimes at the stimulation intensity used in *E1* and *E2,* and more consistently at higher stimulation intensities, an antidromic action potential was evoked. This cell had a resting membrane potential of −59 mV, input resistance of 50 mΩ, and action potential amplitude of 78 mV. Action potentials are truncated in the figure.

ings, to differentiate this cell type from pyramidal cells, basket, and O/A interneurons without the use of intracellular markers (LY or HRP). This should prove an advantage for future physiological studies in which distinctions between these cell types are essential.

Despite the distinctive quality of the cells of stratum lacunosum-moleculare, they share some physiological properties with other CA1 neurons. Similar to pyramidal cells, and in contrast to other interneurons, the action potential amplitude of L-M interneurons is large (60 mV), the action potential duration is long (2.0 msec), the time constant is relatively slow (8.6 msec), there is usually no (or very little) spontaneous firing, and there is typically little evidence of spontaneous synaptic potentials. In common with other interneurons and in contrast to CA1 pyramidal cells, L-M interneuron input resistance is high (64 MΩ), there is a prominent afterhyperpolarization that follows the action potential (in pyramidal cells, a depolarizing afterpotential is seen at this latency), and the cells show very little frequency accommodation during discharge to depolarizing current pulses at resting membrane potential. In contrast to CA1 pyramidal cells and to "basket" and O/A interneurons, L-M interneurons usually display anodal break excitation and change their mode of firing from "sustained" to "burst" type following hyperpolarization of the membrane. These characteristics are

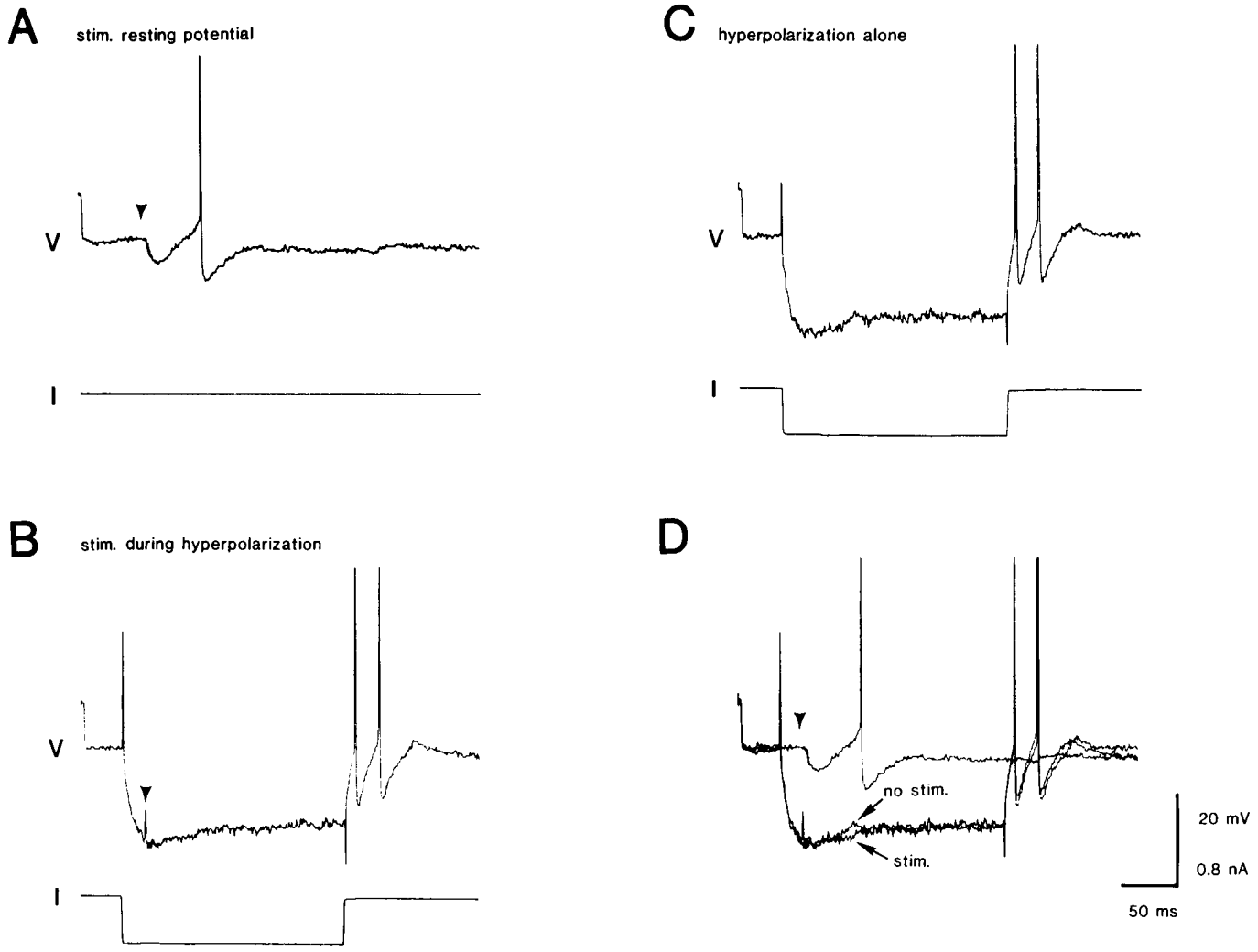

Figure 6. L-M interneuron synaptic responses in a longitudinal slice at resting membrane potential and during membrane hyperpolarization. *A,* Stimulation of stratum oriens (*arrowhead,* 0.4 mA, 0.05 msec) evoked an IPSP followed by a depolarization that triggered an action potential. *B,* Same stimulation of stratum oriens (*arrowhead* same as *A*) during hyperpolarization of the membrane to IPSP reversal potential (−0.4 nA, 200 msec) did not produce any observable late postsynaptic potentials. *C,* Hyperpolarization (as in *B*) of the membrane without stimulation of stratum oriens. *D,* Superimposed voltage traces of *A–C* showing the lack of postsynaptic potentials at hyperpolarized membrane levels. This result indicates that the depolarization following the IPSP arose from intrinsic membrane properties activated by the IPSP, and not from a neurotransmitter-induced EPSP. Same cell as Figure 5 (action potentials truncated).

similar to those previously reported for thalamic neurons and have been suggested to reflect a low-threshold, voltage-dependent calcium conductance (Llinás and Jahnsen, 1982; Jahnsen and Llinás, 1984a, b). Although the functional relevance of these characteristics is not yet clear, it is interesting to note that a depolarizing current pulse of a given amplitude will often evoke more action potentials in the burst mode (when the membrane is hyperpolarized) than in the sustained mode (when the membrane is at normal resting potential) (see Fig. 2, for example).

Morphologically, L-M interneurons were clearly different from pyramidal cells and basket and O/A interneurons. They are morphologically quite homogenous, thus appearing to constitute a single category of interneuron. Interestingly, in a number of interneurons, dendrites were observed crossing the hippocampal fissure and entering stratum moleculare of the dentate gyrus. Although L-M interneurons receive the majority of their afferents from fibers in the CA1 region, they also receive afferents from axons in the dentate gyrus, as shown by our stimulation experiments. The interneuron axon projects for relatively long distances along stratum lacunosum-moleculare but also branches profusely, giving off collaterals that descend into stratum radiatum, pyramidale, and sometimes reach into stratum oriens. In some L-M interneurons, we observed axon collaterals ascending toward the hippocampal fissure (Fig. 3*C,* for example), entering the molecular layer of the dentate gyrus, and projecting toward the dentate granule cell layer. Thus, the L-M interneurons not only send axonal projections to neurons in the CA1 region but also to cells in the dentate gyrus.

Given the morphological characteristics we have observed, it is difficult to identify these LY-filled interneurons within the classification of Ramon y Cajal (1911) and/or Lorente de No (1934), although they are generally similar to L-M interneurons filled with LY in the CA3 region by Misgeld and Frotscher (1986). From the morphology of their soma and dendrites, the L-M interneurons appear similar to Ramon y Cajal's stellate cells of stratum lacunosum (Ramon y Cajal, 1911; fig. 476, m). However, according to Ramon y Cajal, the axon of stellate cells remains in strata lacunosum and moleculare; in contrast, the

axon of L-M interneurons arborizes in strata lacunosum-moleculare, radiatum, pyramidale, and sometimes oriens. Ramon y Cajal also described stratum lacunosum interneurons whose axons descend to the pyramidal layer; however, unlike L-M interneurons, these cells with descending axons have a triangular soma with a different dendritic branching pattern than L-M interneurons (Ramon y Cajal, 1911; fig. 476, g). Similarly, Lorente de No has described stellate interneurons, but their axons remain in strata radiatum and lacunosum (Lorente de No, 1934; fig. 7, cells 6 and 7) in contrast to the axon of L-M interneurons that enters strata pyramidale and sometimes oriens.

The hitherto undescribed presence of dendritic and axonal branches of L-M interneurons reaching into both CA1 and dentate gyrus suggests that these interneurons are responsive to neuronal inputs to both hippocampal regions and, in turn, influence neuronal activity in both CA1 and dentate regions. These dual afferent and efferent connections with CA1 and dentate gyrus appear so far to be a unique characteristic of L-M interneurons since other interneurons whose somata lie in the CA1 region have not been reported to have axonal or dendritic branches outside of this region (Ramon y Cajal, 1911; Lorente de No, 1934; Ribak et al., 1978; Schwartzkroin and Mathers, 1978; Somogyi et al., 1983; Frotscher et al., 1984; Schwartzkroin and Kunkel, 1985).

Results of stimulation experiments indicate that L-M interneurons receive excitatory as well as inhibitory synaptic inputs. However, excitatory synaptic responses are seen when major hippocampal afferents are stimulated in transversely cut slices, whereas inhibitory synaptic inputs are predominantly activated when afferents are stimulated in longitudinally cut slices. The differential nature of synaptic responses in transverse versus longitudinal slices suggests a highly laminated excitatory projection system oriented in the "classic" lamellar fashion onto L-M interneurons and a more diffuse inhibitory system oriented longitudinally across lamellae impinging upon these interneurons.

In transverse slices, electrical stimulation of all layers of CA1 region elicited EPSPs in L-M interneurons, usually of sufficient amplitude to reach threshold and often produce a burst of action potentials. However, the relative efficacy of stimulation of each layer in eliciting EPSPs and action potentials varied across layers and was found to reflect the density of dendritic arborization seen in LY-filled -M interneurons in each layer. Thus, strongest excitatory synaptic responses were elicited from stimulation of stratum lacunosum-moleculare. Smaller amplitude EPSPs and/or fewer action potentials were evoked (in descending order) from strata radiatum > oriens > alveus. Stimulation of stratum moleculare of dentate gyrus was also effective in evoking an EPSP in L-M interneurons, often of sufficient amplitude to elicit an action potential. This excitatory synaptic input from dentate gyrus did not arise from stimulating the trisynaptic circuit, granule cell–CA3 pyramidal (CA1 pyramidal)-interneuron since direct stimulation of CA3 area evoked synaptic responses of much smaller amplitude (e.g., Fig. 4). These electrophysiological results suggest that afferent fibers in the dentate gyrus make excitatory synapses with L-M interneurons, possibly on L-M dendrites such as those we have observed traversing the hippocampal fissure and entering stratum moleculare of dentate gyrus.

In contrast to excitatory synaptic responses elicited in transverse slices, stimulation of major hippocampal afferents in longitudinal slices evoked predominantly inhibitory responses. However, these responses could be quite complex, consisting of hyperpolarization–depolarization–hyperpolarization sequences. The precise nature of the response was more dependent on stimulus intensity than on location of the stimulating electrode; IPSPs of similar amplitude could be evoked from different CA1 layers at similar stimulation intensities. Although a depolarization often followed the stimulus-evoked IPSP in these slices, this later depolarization does not appear to be of synaptic origin since hyperpolarization of the membrane at reversal potential for the IPSP did not uncover the underlying EPSP (Fig. 6). It appears, rather, that the depolarizing oscillations arise from intrinsic membrane conductances activated during the hyperpolarizing potential (IPSP). This membrane conductance could be similar to those producing the anodal break excitation and/or the membrane rectification seen with hyperpolarizing current pulses.

The role of these L-M interneurons in hippocampal circuitry remains unknown. Since some interneurons in stratum lacunosum-moleculare are immunoreactive for the inhibitory neurotransmitter GABA (Gamrani et al., 1986) and its synthesizing enzyme GAD (Somogyi et al., 1984; Kunkel et al., 1986), and since L-M interneurons are strongly excited by major hippocampal afferents, they may mediate feedforward inhibition of CA1 cells. The functional significance of the L-M interneuron membrane properties is also unclear. These conductances result in rebound excitation following strong inhibition. Such intrinsic membrane properties could contribute to the oscillations of the theta rhythm (Green et al., 1960) that are typical of hippocampus. The L-M interneurons with their apparent cholinergic innervation of septal origin (Matthews et al., 1987) and their widespread connections would be ideally suited to help synchronize pyramidal cell populations participating in theta oscillations. Another cell population with a similar intrinsic low threshold conductance, the thalamocortical neurons (Jahnsen and Llinás, 1984a) are critical in the generation of spindling and alpha wave generation typical of thalamocortical circuitry (Ganes and Andersen, 1975).

References

Amaral, D. G. (1978) A Golgi study of cell types in the hilar region of the hippocampus in the rat. J. Comp. Neurol. *182:* 851-914.

Andersen, P., G. N. Gross, T. Lømo, and O. Sveen (1969) Participation of inhibitory and excitatory interneurones in the control of hippocampal cortical output. In *The Interneuron,* M. B. Brazier, ed., pp. 415–432, University of California Press, Berkeley.

Ashwood, T. J., B. Lancaster, and H. V. Wheal (1984) In vivo and in vitro studies of putative interneurones in the rat hippocampus: Possible mediators of feed-forward inhibition. Brain Res. *293:* 279–291.

Buzsaki, G., and E. Eidelberg (1982) Direct afferent excitation and long-term potentiation of hippocampal interneurons. J. Neurophysiol. *48:* 597–607.

Frotscher, M., C. Léránth, K. Lübbers, and W. H. Oertel (1984) Commissural afferents innervate glutamate decarboxylase immunoreactive non-pyramidal neurons in the guinea pig hippocampus. Neurosci. Lett. *46:* 137–143.

Gamrani, H., B. Onteniente, P. Seguela, M. Geffard, and A. Calas (1986) Gamma-aminobutyric acid-immunoreactivity in the rat hippocampus. A light and electron microscopic study with anti-GABA antibodies. Brain Res. *364:* 30–38.

Ganes, T., and P. Andersen (1975) Barbiturate spindle activity in functionally corresponding thalamic and cortical somato-sensory areas in the cat. Brain Res. *98:* 457–472.

Green, J. D., D. S. Maxwell, W. J. Schindler, and C. Stumpf (1960) Rabbit EEG "theta" rhythm: Its anatomical source and relation to activity in single neurons. J. Neurophysiol. *23:* 403–420.

Jahnsen, H., and R. Llinás (1984a) Electrophysiological properties of

guinea-pig thalamic neurones: An in vitro study. J. Physiol. (Lond.) *349:* 205–226.

Jahnsen, H., and R. Llinás (1984b) Ionic basis for the electroresponsiveness and oscillatory properties of guinea-pig thalamic neurones in vitro. J. Physiol. (Lond.) *349:* 227–247.

Knowles, W. D., and P. A. Schwartzkroin (1981) Local circuit synaptic interactions in hippocampal brain slice. J. Neurosci. *1:* 318–322.

Kunkel, D. D., A. E. Hendrickson, J. Y. Wu, and P. A. Schwartzkroin (1986) Glutamic acid decarboxylase (GAD) immunocytochemistry of developing rabbit hippocampus. J. Neurosci. *6:* 541–552.

Lacaille, J.-C., A. L. Mueller, D. D. Kunkel, and P. A. Schwartzkroin (1987) Local circuit interactions between oriens/alveus interneurons and CA1 pyramidal cells in hippocampal slices: Electrophysiology and morphology. J. Neurosci. *7:* 1979–1993.

Llinás, R., and H. Jahnsen (1982) Electrophysiology of mammalian thalamic neurones in vitro. Nature *297:* 406–408.

Lorente de No, R. (1934) Studies on the structure of the cerebral cortex. II. continuation of the study of the ammonic system. J. Psychol. Neurol. (Lpz.) *46:* 113–177.

Matthews, D. A., P. M. Salvaterra, G. D. Crawford, C. R. Houser, and J. E. Vaughn (1987) An immunocytochemical study of choline acetyltransferase-containing neurons and axon terminals in normal and partially deafferented hippocampal formation. Brain Res. *402:* 30–43.

Misgeld, U., and M. Frotscher (1986) Postsynaptic-gabaergic inhibition of non-pyramidal neurons in the guinea-pig hippocampus. Neuroscience *19:* 193–206.

Ramon y Cajal, S. (1911) *Histologie du Systeme Nerveux de l'Homme et des Vertebres,* Maloine, Paris.

Ribak, C. E., J. E. Vaughn, and K. Saito (1978) Immunocytochemical localization of glutamic acid decarboxylase in neuronal somata following colchicine inhibition of axonal transport. Brain Res. *140:* 321–332.

Schwartzkroin, P. A. (1975) Characteristics of CA1 neurons recorded intracellularly in the hippocampal in vitro slice preparation. Brain Res. *85:* 423–436.

Schwartzkroin, P. A. (1981) To slice or not to slice. In *Electrophysiology of Isolated Mammalian CNS Preparations,* G. Kerkut and H. Wheal, eds., pp. 15–50, Academic, London.

Schwartzkroin, P. A., and D. D. Kunkel (1985) Morphology of identified interneurons in the CA1 regions of guinea pig hippocampus. J. Comp. Neurol. *232:* 205–218.

Schwartzkroin, P. A., and C. H. Mathers (1978) Physiological and morphological identification of a nonpyramidal hippocampal cell type. Brain Res. *157:* 1–10.

Somogyi, P., A. D. Smith, M. G. Nunzi, A. Gorio, H. Takagi, and J. Y. Wu (1983) Glutamate decarboxylase immunoreactivity in the hippocampus of the cat: Distribution of immunoreactive synaptic terminals with special reference to the axon initial segment of pyramidal neurons. J. Neurosci. *3:* 1450–1468.

Stewart, W. W. (1978) Functional connections between cells as revealed by dye-coupling with a highly fluorescent naphthalimide tracer. Cell *14:* 741–759.

Wong, R. K. S., D. A. Prince, and A. I. Basbaum (1979) Intradendritic recordings from hippocampal neurons. Proc. Natl. Acad. Sci. USA *76:* 986–990.